

This document is downloaded from DR-NTU, Nanyang Technological University Library, Singapore.

Title	A High-performance compact photoacoustic tomography system for in vivo small-animal brain imaging
Author(s)	Upputuri, Paul Kumar; Periyasamy, Vijitha; Kalva, Sandeep Kumar; Pramanik, Manojit
Citation	Upputuri, P. K., Periyasamy, V., Kalva, S. K., & Pramanik, M. (2017). A High-performance Compact Photoacoustic Tomography System for In Vivo Small-animal Brain Imaging. <i>Journal of Visualized Experiments</i> , (124), e55811-.
Date	2017
URL	<a href="http://hdl.handle.net/10220/43771">http://hdl.handle.net/10220/43771</a>
Rights	© 2017 Journal of Visualized Experiments. This paper was published in <i>Journal of Visualized Experiments</i> and is made available as an electronic reprint (preprint) with permission of <i>Journal of Visualized Experiments</i> . The published version is available at: [ <a href="http://dx.doi.org/10.3791/55811">http://dx.doi.org/10.3791/55811</a> ]. One print or electronic copy may be made for personal use only. Systematic or multiple reproduction, distribution to multiple locations via electronic or other means, duplication of any material in this paper for a fee or for commercial purposes, or modification of the content of the paper is prohibited and is subject to penalties under law.

## Video Article

# A High-performance Compact Photoacoustic Tomography System for *In Vivo* Small-animal Brain Imaging

Paul Kumar Upputuri<sup>1</sup>, Vijitha Periyasamy<sup>1</sup>, Sandeep Kumar Kalva<sup>1</sup>, Manojit Pramanik<sup>1</sup><sup>1</sup>School of Chemical and Biomedical Engineering, Nanyang Technological UniversityCorrespondence to: Manojit Pramanik at [manojit@ntu.edu.sg](mailto:manojit@ntu.edu.sg)URL: <https://www.jove.com/video/55811>DOI: [doi:10.3791/55811](https://doi.org/10.3791/55811)Keywords: Bioengineering, Issue 124, Photoacoustic tomography, small-animal imaging, high-speed imaging, pulsed laser diode, *in vivo* brain imaging, biomedical imaging

Date Published: 6/21/2017

Citation: Upputuri, P.K., Periyasamy, V., Kalva, S.K., Pramanik, M. A High-performance Compact Photoacoustic Tomography System for *In Vivo* Small-animal Brain Imaging. *J. Vis. Exp.* (124), e55811, doi:10.3791/55811 (2017).

## Abstract

*In vivo* small-animal imaging has an important role to play in preclinical studies. Photoacoustic tomography (PAT) is an emerging hybrid imaging modality that shows great potential for both preclinical and clinical applications. Conventional optical parametric oscillator-based PAT (OPO-PAT) systems are bulky and expensive and cannot provide high-speed imaging. Recently, pulsed-laser diodes (PLDs) have been successfully demonstrated as an alternative excitation source for PAT. Pulsed-laser diode PAT (PLD-PAT) has been successfully demonstrated for high-speed imaging on photoacoustic phantoms and biological tissues. This work provides a visualized experimental protocol for *in vivo* brain imaging using PLD-PAT. The protocol includes the compact PLD-PAT system configuration and its description, animal preparation for brain imaging, and a typical experimental procedure for 2D cross-sectional rat brain imaging. The PLD-PAT system is compact and cost-effective and can provide high-speed, high-quality imaging. Brain images collected *in vivo* at various scan speeds are presented.

## Video Link

The video component of this article can be found at <https://www.jove.com/video/55811/>

## Introduction

Photoacoustic tomography (PAT) is a hybrid imaging modality that has many applications in both clinical and preclinical studies<sup>1,2,3,4,5</sup>. In PAT, nanosecond laser pulses irradiate biological tissue. The absorption of incident light by the tissue chromophores leads to a local temperature rise, which then yields pressure waves emitted in the form of sound waves. An ultrasound detector collects the photoacoustic signals at various positions around the sample. The photoacoustic (PA) signals are reconstructed using various algorithms (such as a delay-and-sum algorithm)<sup>6</sup> to generate the photoacoustic image.

This hybrid imaging modality offers high-resolution, deep-tissue imaging and high optical absorption contrast<sup>7,8</sup>. Recently, a ~12-cm imaging depth<sup>9</sup> was achieved in chicken breast tissue with the aid of a longer wavelength (~1,064 nm) and an exogenous contrast agent called phosphorus phthalocyanine. This depth sensitivity is much higher than the depth sensitivity of other optical methods, such as confocal fluorescence microscopy, two-photon fluorescence microscopy,<sup>10</sup> optical coherence tomography,<sup>11</sup> etc. Using more than one wavelength, PAT can demonstrate structural and functional changes in organs. For many human diseases, small-animal models have been well-established<sup>12,13,14,15</sup>. For the imaging of small animals, several modalities have been demonstrated. Out of all those approaches, PA imaging has gained attention rather quickly due to the advantages mentioned above. PAT has shown its potential for imaging blood vessels in the tissues and organs (*i.e.*, heart, lungs, liver, eyes, spleen, brain, skin, spinal cord, kidney, etc.) of small animals<sup>4,16,17,18</sup>. PAT is a well-established modality for small-animal brain imaging. PA waves are produced due to the light absorption by the chromophores, so multiple-wavelength PAT allows for the mapping of total hemoglobin concentration (HbT) and oxygen saturation (SO<sub>2</sub>)<sup>19,20,21,22</sup>. Brain neurovascular imaging was achieved with the aid of exogenous contrast agents<sup>12,23,24</sup>. PA modality can help to give a better understanding of brain health by providing information at the molecular and genetic levels.

For small-animal imaging, Nd : YAG/OPO lasers are widely used as PAT excitation sources. These lasers deliver ~5 ns near-infrared pulses with energy (~100 mJ at the OPO output window) at a ~10-Hz repetition rate<sup>25</sup>. The PA system equipped with such lasers is costly and bulky and allows for low-speed imaging with single-element ultrasound transducers (UST) due to the low repetition rate of the laser source. A typical A-line acquisition time in such PA systems is ~5 min per cross-section<sup>25</sup>. An imaging system with such a lengthy measurement time is not ideal for small-animal imaging, because it is difficult to control the physiological parameters for full-body imaging, time-resolved functional imaging, etc. By adopting multiple single-element USTs, array-based USTs, or a high-repetition-rate laser, it is possible to increase the imaging speed of PA systems. Using only one single-element UST to collect all PA signals around the sample will limit the imaging speed of the system. Multiple single-element USTs arranged in circular or semi-circular geometry are demonstrated for high-speed, highly sensitive imaging techniques. Array-based USTs<sup>26</sup>, such as linear, semi-circular, circular, and volumetric arrays, have been successfully used for real-time imaging<sup>1</sup>. These array-

based USTs will increase the imaging speed and reduce the measurement sensitivity, but they are expensive. However, the imaging speed of PA systems that use array-based USTs is still limited by the repetition rate of the laser.

Pulsed-laser technology advanced to make high-repetition-rate pulsed-laser diodes (PLDs). 7,000 frames/s B-scan photoacoustic imaging was demonstrated with PLDs using a clinical ultrasound platform<sup>27</sup>. Such PLDs can improve the imaging speed of the PAT system, even with single-element UST circular scanning geometry. Single-element USTs are less expensive and highly sensitive, unlike array-based USTs. Over the last decade, little research was reported on the use of high-repetition-rate PLDs as the excitation source for PA imaging. A fiber-based near-infrared PLD was demonstrated for PA imaging of phantoms<sup>28</sup>. The *in vivo* imaging of blood vessels at a ~1 mm depth below the human skin was demonstrated using low-energy PLDs<sup>29</sup>. A PLD-based optical resolution photoacoustic microscope (ORPAM) was reported. Using PLDs, ~1.5 cm deep imaging at a frame rate of 0.43 Hz was demonstrated<sup>30</sup>. Very recently, a PLD-PAT system was reported that provided images in as short as ~3 s and at a ~2 cm imaging depth in biological tissue<sup>25,31</sup>. This study proved that such a low-cost, compact system can provide high-quality images, even at high speeds. The PLD-PAT system can be used for high-frame-rate (7,000 fps) photoacoustic imaging, surficial blood vessel imaging, finger joint imaging, 2 cm-deep tissue imaging, small-animal brain imaging, etc. The single-wavelength and low-pulse-energy pulses from PLD limit its application to multi-spectral and deep-tissue imaging. Experiments have been carried out on small animals using the same PLD-PAT system used for pre-clinical applications. The purpose of this work is to provide the visualized experimental demonstration of the PLD-PAT system for *in vivo* 2D cross-sectional brain imaging of small animals.

## Protocol

All animal experiments were performed according to the guidelines and regulations approved by the Institutional Animal Care and Use Committee of Nanyang Technological University, Singapore (Animal Protocol Number ARF-SBS/NIE-A0263).

### 1. System Description

1. Mount the PLD inside the circular scanner, as shown in **Figure 1a**. Connect the PLD to the laser driver unit (LDU).  
NOTE: The PLD provides ~136-ns pulses at a wavelength of ~803 nm, with a maximum pulse energy of ~1.42 mJ and a repetition rate up to 7 kHz. The laser driving unit (LDU) includes: a temperature controller, a variable power supply, a power supply (12 V), and a function generator; see the Table of Materials. The variable power supply is used to control the laser power, and the function generator is used to change the repetition rate of the PLD.
2. Switch on the PLD laser. Set the PLD repetition rate to "7,000" Hz by using the function generator in the LDU. Increase the pulse energy to 1.42 mJ by setting the voltage of the variable power supply to "3.1" V.
3. Mount the optical diffuser (OD) in front of the PLD exit window to make the output beam homogenous, as shown in **Figure 1a**.  
NOTE: Use a diffuser with a fine grit (*i.e.*, 1,500-grit polish).
4. Mount the focused UST on the UST holder, such that it faces the center of the scanning area, as shown in **Figure 1a**.  
NOTE: The central frequency of the UST is 2.25 MHz, and the focal length is 1.9 in.
5. Place the ultrasound detector inside the acrylic tank, as shown in **Figure 1a**. Fill the tank with water such that the UST is totally immersed.  
NOTE: A water medium is used to couple the photoacoustic signal from the brain (sample) to the UST. An acrylic water tank (WT; see the Table of Materials) was custom-designed for small-animal imaging. The schematic of the water tank design is shown in **Figure 1b**.
6. Check the PA signal from the sample using a pulser/receiver unit (PRU; see the **Table of Materials**).  
NOTE: These signals were digitized by a 12-bit DAQ card (see the **Table of Materials**) at a 100 MS/s sampling rate and were saved on a computer.

### 2. Animal Preparation for Rat Brain Imaging

NOTE: The PLD-PAT system described above was demonstrated for imaging small animal brains. For these experiments, healthy female rats (see the **Table of Materials**) were used.

1. Anesthetize the animal by intraperitoneally injecting a cocktail of 2 mL of ketamine, 1 mL of xylazine, and 1 mL of saline (dosage of 0.2 mL/100 g).
2. Remove the fur on the scalp of the animal using a hair clipper. Gently apply hair removal cream to the shaved area for further depletion of the fur.
  1. Remove the applied cream after 4-5 min using a cotton swab.
  2. Apply artificial tear ointment to the eyes of the animal to prevent the dryness due to anesthesia and laser illumination.
3. Mount the custom-made animal holder (see the **Table of Materials**) equipped with a breathing mask (see the **Table of Materials**) on a lab-jack.
4. Place the animal in prone position on the holder. Secure it to the holder using surgical tape to avoid movement of the animal during imaging.
5. Ensure that the breathing mask covers the nose and mouth of the rat to deliver inhaled anesthetic.

### 3. In Vivo Rat Brain Imaging

1. **Connect the breathing mask to the anesthesia machine. Switch on the anesthesia machine and set it to deliver 1.0 L/min of oxygen with 0.75% isoflurane.**
  1. Clamp the pulse oximeter to its tail to monitor the physiological condition of the animal.
2. **Apply a layer of colorless ultrasound gel to the scalp of the rat. Adjust the lab-jack position to the center of the scanner. The breathing mask is customized to suit the imaging window. 10% of the commercially available nose cone is cut then connected to a piece of glove.**

1. Adjust the height of the lab-jack manually so that the imaging plane is at the focus of the UST.
3. Set the parameters in the data acquisition software (see the Table of Materials) as required. Run the data acquisition software program to start acquisition (*i.e.*, imaging).  
NOTE: The program is used to rotate the UST and collect A-line PA signals. The collected A-lines will be saved on the computer.
4. Observe the animal during the entire imaging period and proceed to PAT reconstruction after the imaging is complete.
5. After the data acquisition is over, reconstruct the cross-sectional brain image from the A-lines using the reconstruction software program.
6. Turn off the anesthesia system, remove the animal from the stage, return it to its cage, and monitor it until it regains consciousness.  
NOTE: For example, if the UST is rotated for 5 s, the PLD delivers 35,000 (= 5 × 7,000) pulses and the UST collects 35,000 A-lines. The 35,000 A-lines are reduced to 500 by averaging over 70 signals (after averaging A-lines = 35,000/70 = 500). **Figure 1c** illustrates the illumination of the laser pulses and A-line collection. A reconstruction program based on delay-and-sum back projection algorithm should be used.

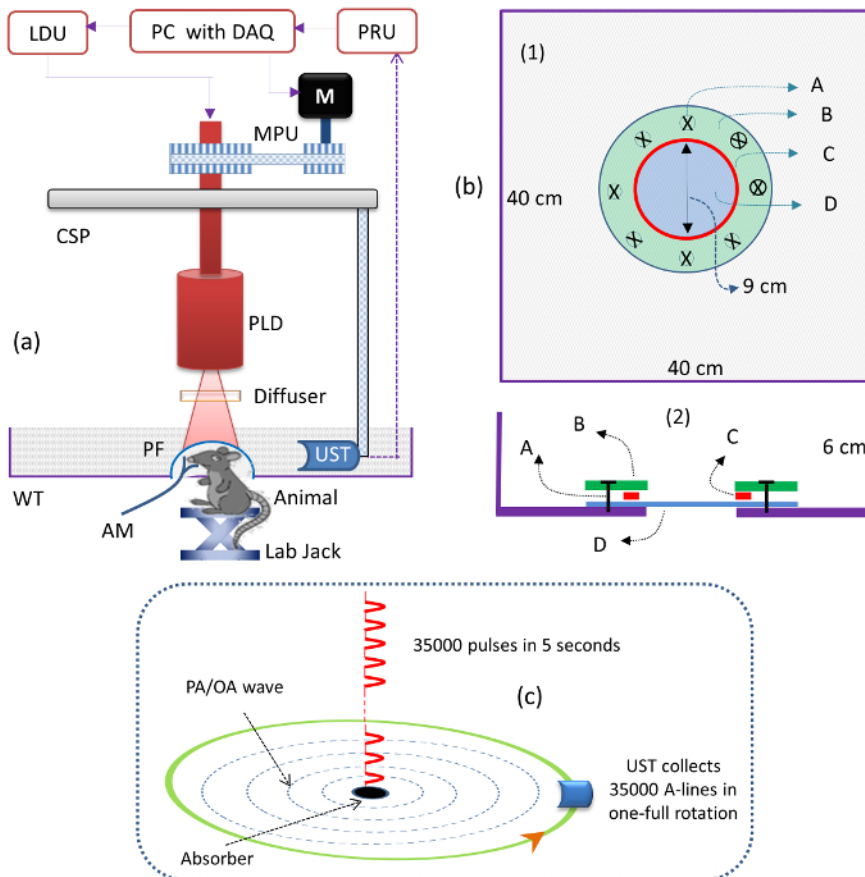


**Figure 1: Schematics of the PLD-PAT System.** (a) Schematic of the PLD-PAT. PLD: pulsed-laser diode, CSP: circular scanning plate, AM: anesthesia machine, M: motor, MPU: motor pulley unit, LDU: laser driver unit, PRU: pulser/receiver unit, UST: ultrasound transducer, WT: water tank, PF: polymer film, and DAQ: data acquisition card. (b) Schematic of the water tank, top view (1) and cross-sectional view (2) for *in vivo* small-animal brain imaging. A: metric Screw, B: acrylic annular plate, C: silicone "O" ring, D: 100 μm-thick, transparent polythene cover. The tank had a 9 cm diameter hole at its bottom and was sealed with an ultrasonically and optically transparent, 100 μm-thick polyethylene membrane. (c) Schematic of the illumination of laser pulses from the PLD and A-lines, collection in a 5 s continuous scan time. [Please click here to view a larger version of this figure.](#)

## Representative Results

The *in vivo* brain imaging results that demonstrate the capabilities of the described PLD-PAT system are showcased in this section. To demonstrate the high-speed imaging capabilities of the PLD-PAT system, the *in vivo* brain imaging of two different healthy rats was performed. **Figure 2** shows the brain images of a female rat (93 g) at various scan speeds. **Figure 2a** and **b** show the photographs of the rat brain before and after removing the scalp over the brain area. PAT imaging was done non-invasively (*i.e.*, with the skin and skull intact). PA signals from the cross-section of the brain were collected by circularly rotating the UST for 5 s, 10 s, 20 s, and 30 s. **Figure 2c-f** show the PAT-reconstructed cross-sectional images of the rat brain, obtained in 5 s, 10 s, 20 s, and 30 s scan times. In all these brain images, the transverse sinus (TS), superior sagittal sinus (SS), and cerebral veins (CV), including branches, are clearly visible. These features are indicated on the image shown in **Figure 2f**. These results promise that the system can provide high-quality *in vivo* images, even at high scanning speeds.

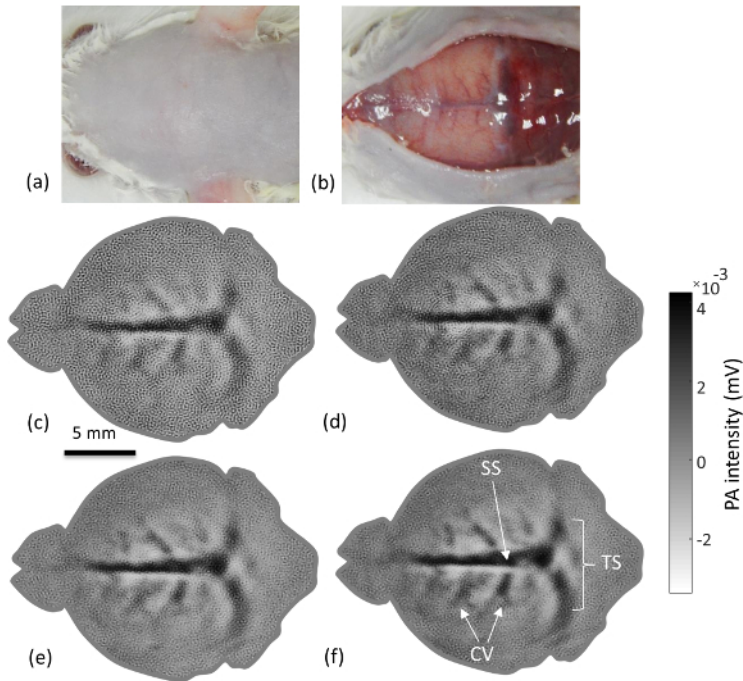


**Figure 2: Non-invasive *In Vivo* PLD-PAT Images.** Non-invasive PLD-PAT images of the vasculature in a 93 g female rat brain. Photograph of the rat brain before (a) and after (b) removing the scalp. *In vivo* brain images at different scan times: (c) 5 s, (d) 10 s, (e) 20 s, and (f) 30 s. SS: sagittal sinus, TS: transverse sinus, and CV: cerebral veins. [Please click here to view a larger version of this figure.](#)

A similar imaging experiment was carried out on another female rat (95 g), and corresponding brain images obtained in 5 s, 10 s, 20 s, and 30 s are shown in **Figure 3**.

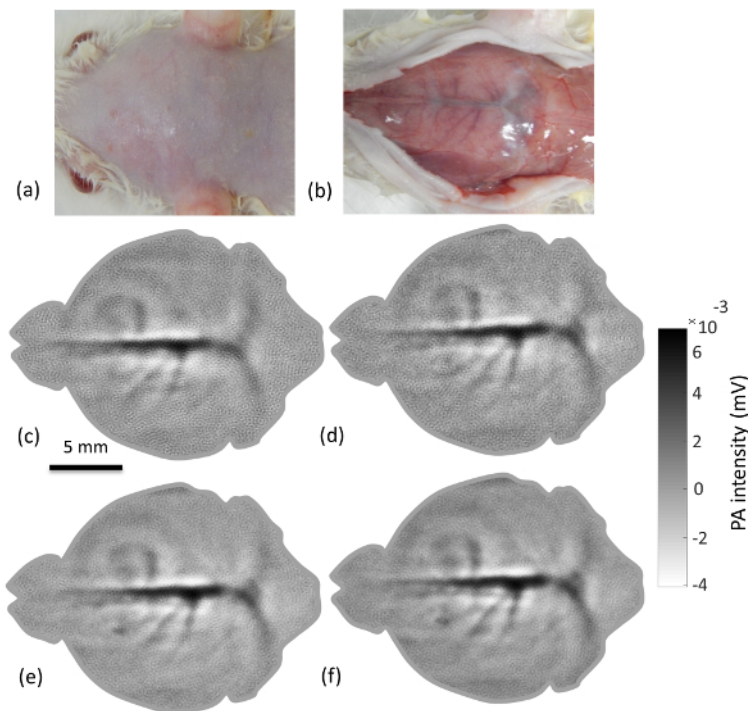


**Figure 3: Non-invasive *In Vivo* PLD-PAT Images.** Non-invasive PLD-PAT images of the vasculature in a 95 g female rat brain. Photograph of the rat brain before (a) and after (b) removing the scalp. *In vivo* brain images at different scan times: (c) 5 s, (d) 10 s, (e) 20 s, and (f) 30 s. [Please click here to view a larger version of this figure.](#)

## Discussion

This work presents a protocol for performing *in vivo* brain imaging on rats using a PLD-PAT system. The protocol includes a detailed description of the imaging system and its alignment, as well as an illustration of brain imaging on rats. The existing OPO-based PAT systems are expensive and bulky and can provide one cross-sectional image in 5-10 min. The PLD-PAT system is compact, portable, and low-cost and can provide good-quality images in 3 s. The performance of the system was previously studied in phantoms and compared with conventional PAT system<sup>25</sup>. Here, the same PLD-PAT was demonstrated for fast *in vivo* brain imaging. The outcome demonstrates that the system can provide high-quality *in vivo* images, even in 5 s.

While there are several advantages, the PLD-PAT system has several drawbacks. The PLD used in this study provides pulses at a single wavelength, so it cannot provide functional imaging, which requires multi-wavelength illumination. For functional imaging, a PLD with multi-wavelength illumination capabilities is required. The low-energy PLD pulses limit the imaging depth. However, using an exogenous contrast agent, it is possible to enhance the imaging depth of the PLD-PAT system.

Usually, the PLD laser beam is not uniform, so a suitable optical diffuser can be used in front of the laser window to improve the image quality. Make sure that the center of the laser beam and the center of the imaging area coincide. While scanning the UST around the brain, ensure that the UST always faces the scan center. When implementing the protocol, additional care needs to be taken: (a) the amount of anesthesia cocktail should be administered according to the weight of the animal; (b) the anesthesia injection must be precise so that the organs (e.g., the urinary bladder, intestine, and kidney) are not affected; (c) during the hair clipping, ensure that the scalp of the animal is not scratched; (d) the pressure of the water tank on the animal must be as minimal as possible; and (e) while positioning the animal under the scanner, make sure that the imaging cross-sectional plane of the brain is at the center of the UST. Future applications of the system include brain tumor imaging, imaging different organs in small animals, high-speed imaging in less than 5 s, investigating biomaterials for contrast agents, and therapy applications. Troubleshooting may be required if the image quality is low.

### Laser safety for small-animal *in vivo* imaging

The maximum permissible exposure (MPE) limit for skin depends on several parameters, such as excitation wavelength, pulse width, time of exposure, illuminating area, etc. The MPE limits for *in vivo* imaging are governed by the American National Standards Institute (ANSI)<sup>32</sup>. In the 700 to 1,050 nm wavelength range, the energy density on the skin delivered by a single pulse should be less than  $20 \times 10^{2(\lambda-700)/1,000} \text{ mJ/cm}^2$  ( $\lambda$ : excitation wavelength in nm). For the 803 nm PLD wavelength, the limit is  $\sim 31 \text{ mJ/cm}^2$ . If the laser is used continuously over a period of  $t = 5 \text{ s}$ , then the MPE becomes  $1.1 \times 10^{2(\lambda-700)/1000} \times t^{0.25} \text{ J/cm}^2 (= 2.6 \text{ J/cm}^2)$ . In this experiment, the PLD was operated at 7,000 Hz. In a 5-s scan time, a total of 35,000 ( $5 \times 7,000$ ) pulses were delivered to the sample, so per pulse, the MPE was  $0.07 \text{ mJ/cm}^2$ . In the described imaging system, the PLD delivers pulses with energy at  $\sim 1.05 \text{ mJ}$  per pulse, and the laser beam was expanded over a  $\sim 12.6 \text{ cm}^2$  area. Hence, the laser energy density was  $\sim 0.08 \text{ mJ/cm}^2$  on the brain area. The ANSI laser safety limit of the PAT system can be changed by reducing the laser power, by expanding the laser beam, or by reducing the pulse repetition rate.

## Disclosures

The authors have no relevant financial interests in the manuscript and no other potential conflicts of interest to disclose.

## Acknowledgements

The research is supported by the Tier 2 grant funded by the Ministry of Education in Singapore (ARC2/15: M4020238) and the Singapore Ministry of Health's National Medical Research Council (NMRC/OFIRG/0005/2016: M4062012). The authors would like to thank Mr. Chow Wai Hoong Bobby for the machine shop help.

## References

1. Upputuri, P. K., & Pramanik, M. Recent advances toward preclinical and clinical translation of photoacoustic tomography: a review. *J Biomed Opt.* **22** (4), 041006 (2017).
2. Strohm, E. M., Moore, M. J., & Kolios, M. C. Single Cell Photoacoustic Microscopy: A Review. *IEEE Sel Top Quantum Electron.* **22** (3), 6801215 (2016).
3. Valluru, K. S., & Willmann, J. K. Clinical photoacoustic imaging of cancer. *Ultrasonography.* **35** (4), 267 (2016).
4. Zhou, Y., Yao, J., & Wang, L. V. Tutorial on photoacoustic tomography. *J Biomed Opt.* **21** (6), 061007 (2016).
5. Yao, J., & Wang, L. V. Photoacoustic Brain Imaging: from Microscopic to Macroscopic Scales. *Neurophotonics.* **1** (1), 011003 (2014).
6. Kalva, S. K., & Pramanik, M. Experimental validation of tangential resolution improvement in photoacoustic tomography using a modified delay-and-sum reconstruction algorithm. *J Biomed Opt.* **21** (8), 086011 (2016).
7. Strohm, E. M., Moore, M. J., & Kolios, M. C. High resolution ultrasound and photoacoustic imaging of single cells. *Photoacoustics.* **4** (1), 36-42 (2016).
8. Upputuri, P. K., Wen, Z.-B., Wu, Z., & Pramanik, M. Super-resolution photoacoustic microscopy using photonic nanojets: a simulation study. *J Biomed Opt.* **19** (11), 116003 (2014).
9. Zhou, Y. *et al.* A Phosphorus Phthalocyanine Formulation with Intense Absorbance at 1000 nm for Deep Optical Imaging. *Theranostics.* **6** (5), 688-697 (2016).
10. Upputuri, P. K., Wu, Z., Gong, L., Ong, C. K., & Wang, H. Super-resolution coherent anti-Stokes Raman scattering microscopy with photonic nanojets. *Opt Express.* **22** (11), 12890-12899 (2014).

11. Raghunathan, R., Singh, M., Dickinson, M. E., & Larin, K. V. Optical coherence tomography for embryonic imaging: a review. *J Biomed Opt.* **21** (5), 050902 (2016).
12. Burton, N. C. *et al.* Multispectral opto-acoustic tomography (MSOT) of the brain and glioblastoma characterization. *Neuroimage.* **65** (2), 522-528 (2013).
13. Su, R., Ermilov, S. A., Liopo, A. V., & Oraevsky, A. A. Three-dimensional optoacoustic imaging as a new noninvasive technique to study long-term biodistribution of optical contrast agents in small animal models. *J Biomed Opt.* **17** (10), 101506 (2012).
14. Hu, S., Maslov, K., & Wang, L. V. In vivo functional chronic imaging of a small animal model using optical-resolution photoacoustic microscopy. *Med Phys.* **36** (6), 2320-2323 (2009).
15. Zhang, E. Z., Laufer, J., Pedley, R. B., & Beard, P. 3D photoacoustic imaging system for in vivo studies of small animal models. *Proc SPIE.* **6856** 68560P (2008).
16. Deng, Z., Li, W., & Li, C. Slip-ring-based multi-transducer photoacoustic tomography system. *Opt Lett.* **41** (12), 2859-2862 (2016).
17. Tang, J., Coleman, J. E., Dai, X., & Jiang, H. Wearable 3-D Photoacoustic Tomography for Functional Brain Imaging in Behaving Rats. *Sci Rep.* **6** 25470 (2016).
18. Pramanik, M. *et al.* In vivo carbon nanotube-enhanced non-invasive photoacoustic mapping of the sentinel lymph node. *Phys Med Biol.* **54** (11), 3291-3301 (2009).
19. Yao, J., Xia, J., & Wang, L. V. Multiscale Functional and Molecular Photoacoustic Tomography. *Ultrason Imaging.* **38** (1), 44-62 (2016).
20. Huang, S., Upputuri, P. K., Liu, H., Pramanik, M., & Wang, M. A dual-functional benzobisthiadiazole derivative as an effective theranostic agent for near-infrared photoacoustic imaging and photothermal therapy. *J Mat Chem B.* **4** (9), 1696-1703 (2016).
21. Olefir, I., Mercep, E., Burton, N. C., Ovsepian, S. V., & Ntziachristos, V. Hybrid multispectral optoacoustic and ultrasound tomography for morphological and physiological brain imaging. *J Biomed Opt.* **21** (8), 086005 (2016).
22. Hu, S., Maslov, K., Tsytsarev, V., & Wang, L. V. Functional transcranial brain imaging by optical-resolution photoacoustic microscopy. *J Biomed Opt.* **14** (4), 040503 (2009).
23. Yao, J. J. *et al.* Noninvasive photoacoustic computed tomography of mouse brain metabolism in vivo. *Neuroimage.* **64** (1), 257-266 (2013).
24. Hu, S., & Wang, L. V. Neurovascular photoacoustic tomography. *Front Neuroenergetics.* **2** 10 (2010).
25. Upputuri, P. K., & Pramanik, M. Performance characterization of low-cost, high-speed, portable pulsed laser diode photoacoustic tomography (PLD-PAT) system. *Biomed Opt Express.* **6** (10), 4118-4129 (2015).
26. Yang, X. *et al.* Photoacoustic tomography of small animal brain with a curved array transducer. *J Biomed Opt.* **14** (5), 054007 (2009).
27. Sivasubramanian, K., & Pramanik, M. High frame rate photoacoustic imaging at 7000 frames per second using clinical ultrasound system. *Biomed Opt Express.* **7** (2), 312-323 (2016).
28. Allen, J. S., & Beard, P. Pulsed near-infrared laser diode excitation system for biomedical photoacoustic imaging. *Opt Lett.* **31** (23), 3462-3464 (2006).
29. Kolkman, R. G. M., Steenbergen, W., & van Leeuwen, T. G. In vivo photoacoustic imaging of blood vessels with a pulsed laser diode. *Lasers Med Sci.* **21** (3), 134-139 (2006).
30. Daoudi, K. *et al.* Handheld probe integrating laser diode and ultrasound transducer array for ultrasound/photoacoustic dual modality imaging. *Opt Express.* **22** (21), 26365-26374 (2014).
31. Upputuri, P. K., & Pramanik, M. Pulsed laser diode based optoacoustic imaging of biological tissues. *Biomed Phys Eng Express.* **1** (4), 045010-045017 (2015).
32. American National Standard for Safe Use of Lasers ANSI Z136.1-2000. American National Standards Institute, Inc., New York, NY (2000).